

Mutations of a Residue within the Polyproline-Rich Region of Env Alter the Replication Rate and Level of Cytopathic Effects in Chimeric Avian Retroviral Vectors

Kevin W. Chang,¹ Eugene V. Barsov,² Andrea L. Ferris,¹ and Stephen H. Hughes^{1*}

HIV Drug Resistance Program¹ and AIDS Vaccine Program, SAIC-Frederick,² National Cancer Institute at Frederick, Frederick, Maryland 21702-1201

Received 19 April 2004/Accepted 3 May 2005

Previous attempts to extend the host range of the avian sarcoma/leukosis virus (ASLV)-based RCASBP vectors produced two viral vectors, RCASBP M2C (4070A) and RCASBP M2C (797-8), which replicate using the amphotropic murine leukemia virus 4070A Env protein (2). Both viruses were adapted to replicate efficiently in the avian cell line DF-1, but RCASBP M2C (4070A) caused extensive cytopathic effects (CPE) in DF-1 cells whereas RCASBP M2C (797-8) induced low levels of CPE. The two viruses differed only at amino acid 242 of the polyproline-rich region in the surface (SU) subunit of the Env protein. In RCASBP M2C (4070A), an isoleucine replaced the wild-type proline residue, whereas a threonine residue was found in RCASBP M2C (797-8). In the present study, we show that other amino acid substitutions at position 242 strongly influence the CPE and replication rate of the chimeric viruses. There was a correlation between the amount of unintegrated linear retroviral DNA present in infected DF-1 cells and the level of CPE. This suggests that there may be a role for superinfection in the CPE. The treatment of RCASBP M2C (4070A)-infected cells with dantrolene, which inhibits the release of calcium from the endoplasmic reticulum (ER), reduced the amount of CPE seen during infection with the highly cytotoxic virus. Dantrolene treatment did not appear to affect virus production, suggesting that Ca²⁺ release from the ER had a role in the CPE caused by these viruses.

The avian sarcoma/leukosis virus (ASLV)-based RCAS and RCAN retroviral vectors have been widely used to study several biological processes, such as cancer, development, and basic retrovirology (8, 23, 24). The vectors are replication competent and accept DNA inserts of up to 2.5 kb. RCASBP vectors express the Bryan high-titer polymerase and replicate to viral titers over 10⁶/ml. The different envelope (Env) proteins (subgroups A to J) found in naturally occurring ASLVs play an important role in determining the host range. The A, B, D, and E *env* genes have been incorporated into RCAS to produce vectors that express these Env proteins. However, none of these Env proteins allows for the efficient infection of unmodified mammalian cells. The two current solutions to this problem are (i) mammalian cell lines modified to express the *tva* or *tvb* receptor (3) and (ii) RCAS viruses modified to replicate using an envelope protein from a murine retrovirus (1, 2).

We previously generated the RCASBP-based chimeric vectors RCASBP (Eco) and RCASBP M2C (4070A), which carry and express the *env* genes from the ecotropic murine leukemia virus and amphotropic murine leukemia virus (MLV) 4070A, respectively (1, 2). The original RCASBP M(4070A) parental clone replicated poorly in chicken embryonic fibroblasts (CEF). Serial passages in CEF produced an adapted virus, RCASBP M2C (4070A) (Fig. 1). This variant replicated well in both CEF and DF-1, an immortalized CEF cell line (13, 28). RCASBP M2C (4070A) had a single amino acid substitution,

P242I, in the surface (SU) subunit of *env* and was extremely cytotoxic to CEF. Syncytia, extensive vacuolization, and cell death are seen in cells infected with RCASBP M2C (4070A). In order to select for a virus that was less cytotoxic, RCASBP M2C (4070A) was passaged in chicken embryos. A virus, RCASBP M2C (797-8), was isolated that caused low cytopathic effects (CPE) in DF-1 cells but maintained the ability to replicate efficiently (2). In RCASBP M2C (797-8), the isoleucine residue at position 242 was mutated to threonine (Fig. 1). Proline 242 lies within the highly conserved N-terminal end of the polyproline-rich region (PRR) in SU. The PRR connects the N-terminal and C-terminal domains of SU (26). This region has been shown to influence the conformational stability of SU and to affect the interactions between SU and TM (10, 16, 33). Virus-cell and cell-cell fusion mediated by the murine Env protein can be affected by mutations within the PRR (16, 17, 20).

In the ASLV system, from which the RCASBP vectors are derived, infections by subgroup B, D, and F viruses induce CPE in cultured avian cells, whereas infections by subgroup A, C, and E viruses typically do not. The receptor for subgroup B, D, and E viruses is CAR1 (now called *tvb*), which appears to be a member of the tumor necrosis factor receptor family. *tvb* carries a “death domain,” and it has been proposed that the CPE caused by the subgroup B and D viruses results from activation of the *tvb* receptor (5, 6). Retroviruses can cause CPE by other mechanisms. For retroviruses of the spleen necrosis virus family, a correlation was found between viruses that induced CPE in certain cell types and an accumulation of unintegrated linear viral DNA during acute infection (15). Similar results were obtained with ASLV, and blocking reinfection by the cytopathic viruses with antisera prevented the

* Corresponding author. Mailing address: HIV Drug Resistance Program, NCI-Frederick, P.O. Box B, Bldg. 539, Rm. 130A, Frederick, MD 21702-1201. Phone: (301) 846-1619. Fax: (301) 846-6966. E-mail: hughes@ncifcrf.gov.

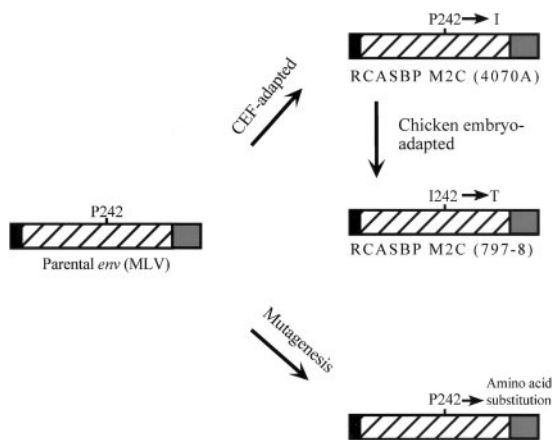


FIG. 1. Schematic of the MLV 4070A Env protein found in the RCASBP M2C-based viruses. Shown are the Env signal sequence (black boxes), the SU subunit (hatched boxes), and the TM subunit (gray boxes). In the chimeric vectors, the signal sequence from the envelope A gene found in RCASBP(A) is retained. Passage of the parental virus, RCASBP M(4070A), in CEF gave rise to a virus, RCASBP M2C (4070A), in which the proline residue found at position 242 of the SU subunit was changed to isoleucine. The passage of RCASBP M2C (4070A) in chicken embryos resulted in a virus that causes low CPE [RCASBP M2C (797-8)], which has I242 mutated to a threonine residue. The amino acid at position 242 was replaced with various amino acids by PCR mutagenesis.

buildup of both linear retroviral DNA and CPE (31). This led to the proposals that superinfection was not completely blocked in the cells in which CPE was seen and that the accumulation of viral DNA might be a cause of the CPE. A link between superinfection and CPE has also been reported for other retroviruses, including human immunodeficiency virus type 1 (HIV-1) (25, 27), feline leukemia virus (21), and mink cell focus-forming murine leukemia virus (34). In most of the reported cases, the cells in which the CPE was seen were not derived from the organism that was the primary host for the virus. This suggests the possibility that when there is an imperfect match between the retroviral Env protein and the receptor, receptor interference may not be complete, allowing superinfection to occur. The large accumulation of unintegrated linear retroviral DNA was postulated to cause some of the CPE by inducing apoptosis in infected cells (18, 34).

Here we report that in RCASBP-based chimeric vectors expressing the MLV 4070A Env protein, the amino acid at position 242 of the SU subunit strongly affects both the replication rate and the level of CPE. A large accumulation of unintegrated linear retroviral DNA was found in cells infected with a highly cytotoxic variant, RCASBP M2C (4070A), supporting a role for superinfection in the CPE. The amount of CPE associated with RCASBP M2C (4070A) infection was reduced by the addition of dantrolene, an inhibitor of calcium release from the endoplasmic reticulum (ER).

MATERIALS AND METHODS

Cell line propagation. DF-1, a cell line derived from chicken embryonic fibroblasts (13, 28), was grown in Dulbecco's modified Eagle's medium (GIBCO) supplemented with 5% newborn calf serum, 5% fetal bovine serum, 100 U of penicillin per ml, and 100 μ g of streptomycin per ml (GIBCO) at 39°C. The cells were passaged at a 1:5 dilution for routine propagation.

Construction of RCASBP M2C plasmids. Plasmids carrying the proviral constructs were mutated using PCR. Overlapping primer extension was used to construct the chimeric amphotropic *env* genes in which the codon for the proline at position 242 was replaced with codons for other amino acids. Two fragments were PCR amplified from RCASBP M2C (4070A) (1). One fragment spanned the unique KpnI site and codon 242 in gp70 and was amplified by using the primers RSV-FOR (5'-GGACGAGGTTATGCCGCTGTG-3') and 242-BACK [5'-TTGGGCCCTAT(NNN)GACTCGGGGTC-3']. The second fragment spanned codon 242 and the remaining downstream open reading frame for gp70 followed by a unique NotI site; the fragment was amplified by using the primers 242-FOR [5'-TGGGACCCCGAG(NNN)TCATAGGGCC-3'] and MLV-BACK (5'-AGCGCCGCTCATGGCTCGTACTCTATGGGTT-3'). These two fragments were fused and amplified by PCR with the primers RSV-FOR and MLV-BACK. The resulting PCR products, which contained the substitution mutations at position 242 of Env, were cleaved with KpnI and NotI. The *env* gene was removed from RCASBP-M2C (4070A) by digestion with KpnI and NotI and replaced with the chimeric mutant KpnI-NotI fragments, generating the mutant vector RCASBP M2C (242-mut). The presence of a correct mutant codon at position 242 was confirmed by DNA sequencing.

The RCANBP M2C (242-mut) CMVgfp plasmids were constructed as follows. The cytomegalovirus (CMV) promoter sequence was PCR amplified from the plasmid template pIRES2-EGFP (Clontech) using the primers 5'-TATTAGCGGCCCATGTCATTAGT-3' (encoding a NotI site) and 5'-CCATCGATGGA TCTGACGGTTCCTACT-3' (encoding a ClaI site). The amplified fragment was digested with NotI and ClaI and ligated into RCASBP M2C (797-8), also digested with NotI and ClaI, to yield RCANBP M2C (797-8)CMV. The enhanced green fluorescent protein (EGFP) gene was removed from RCASBP(A)gfp as a ClaI fragment and ligated into the ClaI site of RCASBP M2C (797-8) CMV. The resulting vector, RCANBP M2C (797-8)CMVgfp, was digested with NotI and MluI to isolate the CMVgfp cassette. CMVgfp was transferred to RCASBP M2C (4070A), (Pro), (Ser), (Gln), and (Thr) as a NotI-MluI fragment.

Transfection and virus production. DF-1 cells seeded at 1.5×10^6 cells per 100-mm plastic culture dish (Falcon) were transfected with 10 μ g of an RCASBP or RCANBP plasmid by the calcium phosphate precipitation method (9). At 4 hours posttransfection, the cells were briefly subjected (5 min) to a glycerol shock with 15% sterile glycerol in culture medium. Following the glycerol shock, the cells were washed twice with $1 \times$ phosphate-buffered saline (PBS) and once with culture medium. For Southern blot experiments, the cells used to generate the viral stocks were washed twice in the manner described above at approximately 16 h and 24 h posttransfection. At 4 days posttransfection, the supernatant was collected and centrifuged for 15 min at 3,000 rpm to remove cellular debris. The clarified supernatant was used to infect fresh DF-1 cells.

Measurement of virus production kinetics. The culture medium was harvested from DF-1 cells transfected with the RCASBP M2C (wild type or 242 mutant) plasmid at various times posttransfection, and the relative amount of virus in the medium was quantified by a p27 antigen-capture enzyme-linked immunosorbent assay (ELISA) as described previously (2). The transfected cells were passaged when they were confluent (every other day) at a 1:5 dilution.

Titration of RCANBP M2C (242-mut)CMVgfp on mammalian cells. Virus stocks were prepared by transfecting DF-1 cells with plasmids expressing RCANBP M2C (4070A), (797-8), (Pro), (Ser), (Gln), or (Thr)CMVgfp and passaging the cells to allow for spread of the virus. Culture supernatants were collected at passage 3 or 4 and centrifuged for 10 min at 3,000 rpm to remove cell debris. Recipient 293 cells plated at 5×10^5 cells per well in six-well tissue culture plates were infected with serial dilutions of the viral stocks. At 48 hours postinfection, the 293 cells were harvested, and GFP expression was quantitated by fluorescence-activated cell sorter (FACS) analysis. The amount of virus in each infection was measured by p27 ELISA, and the percentage of GFP-positive cells was normalized to this value. The relative titer of each virus was expressed as a percentage of the titer of RCANBP M2C (Pro), which carries wild-type MLV 4070A *env*.

Confocal microscopy. DF-1 cells infected with RCASBP M2C (4070A) or one of the 242 mutants were grown in 35-mm plastic culture dishes. Confocal microscopy was performed with an inverted laser confocal microscope (Zeiss, Jena, Germany) at a magnification of $\times 200$.

Cytotoxicity assays. DF-1 cells were infected in the same manner as described for the Southern blot experiments. Each time the cells became confluent, they were removed from the dish with Versene (Invitrogen). An aliquot of the cells was passaged at a 1:5 dilution. The rest of the cells were pooled with the cells present in the washes and collected by centrifugation for 10 min at 1,000 rpm. The cells were resuspended in 2 ml of culture medium. An aliquot of the resuspended cells was then diluted with ViaCount reagent (Guava Technologies) at a 1:20 dilution and incubated for 5 min at room temperature, and the numbers

of viable cells/ml and total cells/ml were determined with a Guava Technologies cell counter.

Env expression and virion incorporation. DF-1 cells were transfected with plasmid DNA carrying the RCASBP M2C vectors, as previously described, and cultured for 4 days at 39°C. The supernatant was collected and clarified by centrifugation at 3,000 rpm for 15 min. The transfected cells were washed once with 1× PBS and then lysed with RIPA buffer (150 mM NaCl, 50 mM Tris, pH 7.4, 0.5% Triton X-100, 0.5% sodium deoxycholate, 0.05% sodium dodecyl sulfate) for 10 min on ice. Cellular debris was removed from the lysate by microcentrifugation for 10 min at 16,000 rpm. An aliquot of the cellular lysate was fractionated in a 4 to 12% polyacrylamide gel (NuPaGE bis-Tris; Invitrogen) and transferred to a nitrocellulose membrane for Western blot analysis. The blots were probed with rabbit anti-gp70 (a kind gift from Alan Rein) at a 1:1,000 dilution, followed by incubation with protein G-biotin (Calbiochem) at a 1:3,000 dilution. Env expression was measured by incubation of the blot with a 1:3,000 dilution of streptavidin-horseradish peroxidase (Amersham Pharmacia) and by ECL (Amersham Pharmacia). The blots were then washed and re probed with rabbit anti-p27 conjugated to horseradish peroxidase (Charles River Laboratories) at a 1:3,000 dilution to measure Gag expression. Virions in the clarified supernatant were isolated by ultracentrifugation of the supernatant through a 15% sucrose cushion for 1 h at 35,000 rpm at 4°C. The viral pellets were resuspended in 4× sample buffer (Invitrogen), fractionated in a 4 to 12% polyacrylamide gel, and transferred to a nitrocellulose membrane for Western blot analysis, using the same protocol described for the cellular lysates.

Sequencing of mutant env genes. The mutant *env* genes were sequenced by the dideoxy chain termination method with primers specific for the amphotropic *env* genes (1).

Southern blotting. DF-1 cells seeded at 2×10^6 cells per 100-mm dish were infected for 24 h at 39°C with virus produced by transfection. Infected cells were passaged every other day at a 1:5 dilution. Linear viral DNAs were extracted from the infected cells at passage 2, at 4 days postinfection, by the method of Hirt (14). The viral DNAs were fractionated in a 1% Tris-acetate-EDTA-agarose gel and transferred by blotting to a nitrocellulose membrane overnight. RCASBP(A) plasmid DNA was digested with *ApaI* and fractionated in the gel as a size reference. The blot was probed with [α - 32 P]dCTP-labeled DNA fragments (Prime-It II; Stratagene) generated by *NcoI* and *XhoI* restriction digestion of the 7.3-kb *PvuI* fragment from RCASBP(A) by overnight hybridization at 41°C on a platform rocker. The blot was washed twice with $2 \times$ SSC ($1 \times$ SSC is 0.15 M NaCl plus 0.015 M sodium citrate), and autoradiography was performed.

FACS analysis of cell surface Env expression. DF-1 cells were infected in the same manner as described for the Southern blot experiments. Cell staining was performed essentially as described by Lu and Roth (19). At passage 2, 1×10^6 infected cells were resuspended in 250 μ l of 1× PBS and stained with the rat monoclonal antibody 83A25 (7) at a 1:100 dilution for 1 h on ice. The cells were washed twice with 1× PBS and stained with a fluorescein isothiocyanate-labeled goat anti-rat polyclonal antibody (BioSource) at a 1:50 dilution for 1 h on ice. The stained cells were analyzed for cell surface Env expression by FACS analysis using a Beckman Coulter EpicsXL-MCL machine.

Dantrolene treatment. DF-1 cells were infected with the RCASBP M2C (4070A) virus generated by transfection, as described for the Southern blot experiments. After passage 1 or at 2 days postinfection, 3×10^5 cells were seeded onto 35-mm glass-bottom culture dishes (Mat-Tek Corp.) and treated with 50 μ M dantrolene (Sigma-Aldrich, Inc.) that had been resuspended in distilled water and sterilized by passage through a 0.22- μ m syringe filter. The culture medium and dantrolene were replaced every other day for 3 days. An aliquot of the culture medium was taken at 4 days posttreatment for the p27 antigen-capture ELISA. The untreated controls were processed in a manner similar to the treated samples. Images of untreated and treated cells were taken at 4 days posttreatment using an Olympus CK-40 inverted microscope at a magnification of $\times 200$.

RESULTS

RCASBP M2C (242-mut) vectors replicate at different rates. Previous work with avian cells demonstrated that the replication rate and the amount of CPE caused by the amphotropic MLV Env-expressing RCASBP-based vectors were affected by the amino acid residue at position 242 of the SU subunit (1, 2). To investigate the influence of this amino acid position on the replication and cytotoxicity of these chimeric vectors, we constructed a series of mutant vectors, RCASBP M2C (242-mut),

TABLE 1. RCASBP M2C mutants and phenotypes

Amino acid at position 242	Cytopathic effects	Initial replication rate
Ile	High	High
Glu	High	High
Leu	High	Low
Ala	High	Low
Ser	High	Low
Trp	High	Low
Val	Moderate	High
Lys	Moderate	High
Arg	Moderate	High
Gln	Moderate/High	High
Met	Low	High
Thr	Low	High
Asn	Low	High
Gly	Low	High
His	Low	High
Tyr	Low	High
Pro	Low	Low
Cys	No virus	NA ^a

^a NA, not applicable.

in which the isoleucine codon at position 242 of the RCASBP M2C vector was replaced with codons for different amino acids. The mutants we generated are summarized in Table 1. The vector RCASBP M2C (Pro) expresses the wild-type MLV gp70, while RCASBP M2C (Thr) recreated the low-cytopathogenicity virus RCASBP M2C (797-8), derived by the adaptation of RCASBP M2C (4070A) in chicken embryos.

The rates of replication were determined by transfecting DF-1 cells with the different RCASBP M2C (242-mut) vectors and passaging the cells six times, if possible, to allow the viruses to replicate. In order to compare the replication rates of the mutant vectors and the parental vector RCASBP M2C (4070A), parallel DF-1 cell cultures were transfected with RCASBP M2C (4070A) for each experiment. Cells transfected with RCASBP M2C (4070A) were passaged only three times because of extensive cell death (see Fig. 3). An aliquot of the culture medium was collected at each passage and analyzed for the presence of viral particles using a p27 antigen-capture ELISA. As expected, the control vector RCASBP M2C (4070A) replicated rapidly in DF-1 cells, with viral production reaching peak levels by passage 3 (Fig. 2A). The initial replication rates of the mutated viruses varied dramatically and, in general, fell into two categories, either low or high. The one exception was RCASBP M2C (Cys), which did not replicate in DF-1 cells (data not shown).

An example of a virus that exhibited a low initial replication rate was RCASBP M2C (Pro), which recreated the wild-type 4070A Env (Fig. 2B). After an initial lag phase during the first three passages, virus production increased steadily in subsequent passages, eventually reaching levels of p27 expression comparable to those of RCASBP M2C (4070A). This pattern characterized viruses in this group, although the number of passages spent in lag phase varied among the viruses.

The second group of chimeric viruses exhibited high initial replication rates with no lag phase and had replication rate curves that were similar to that of RCASBP M2C (4070A) (Fig. 2C). As shown for RCASBP M2C (Val) (Fig. 2C), virus

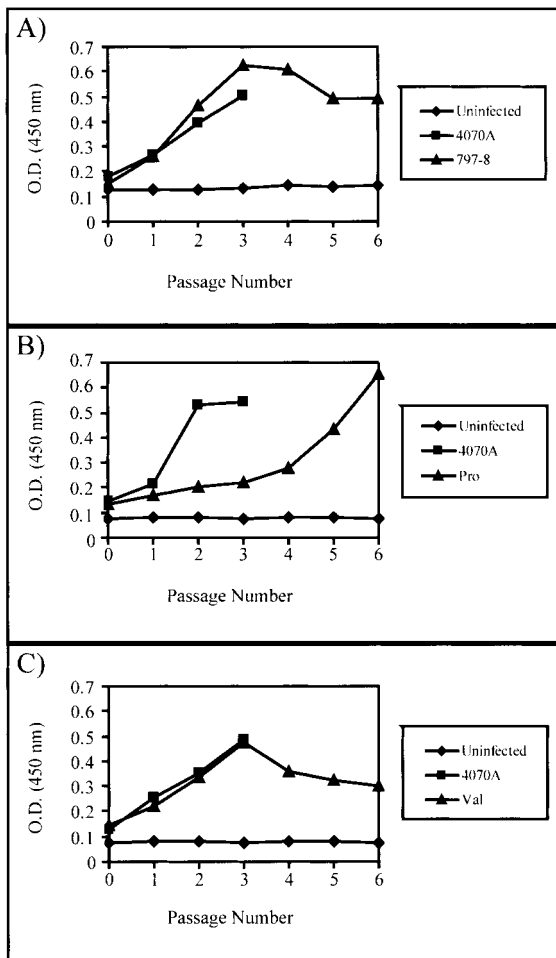


FIG. 2. Representative replication kinetics of RCASBP M2C viruses measured by p27 antigen-capture ELISA. The amounts of p27 antigen found in the supernatants of cells transfected with the various proviral constructs were determined for up to six passages. In parallel, an uninfected negative control (diamonds) and cells transfected with RCASBP M2C (4070A) (squares) were included with each experiment. After passage 3, p27 levels were not determined for RCASBP M2C (4070A)-transfected cells because most of the cells had been lost from the culture (A) RCASBP M2C (4070A) versus (797-8) (triangles) replication kinetics. (B) Virus with low initial replication rate [RCASBP M2C (Pro)] (triangles). (C) Virus with high initial replication rate [RCASBP M2C (Val)] (triangles). At least two independent experiments were performed for each RCASBP M2C variant. O.D., optical density.

production reached a plateau for the rapidly replicating viruses after the initial cell passages.

To determine the replication rates of the viruses generated by passage of the different RCASBP M2C (242-mut)-transfected DF-1 cells, fresh cultures of DF-1 cells were infected with viral stocks collected from the passaged cells. The infected DF-1 cells were passaged, and the amount of virus in the culture supernatant was measured by p27 antigen-capture ELISA, as described above. All of the mutant viruses replicated rapidly with no lag period (data not shown). This suggests that the increase in virus production seen with the chimeric viruses which initially replicated slowly might be due to either a mutation at position 242 or a secondary mutation

TABLE 2. Relative titers of RCANBP M2C viruses in 293 cells^a

Virus	Relative titer (%)
RCANBP M2C (Pro)	100
RCANBP M2C (4070A)	39
RCANBP M2C (Ser)	10
RCANBP M2C (Gln)	0
RCANBP M2C (797-8)	37
RCASBP (A)	0

^a Viruses were titrated on human 293 cells by flow cytometry and normalized to the amount of p27 antigen. The data are the averages of two independent experiments and were normalized relative to RCANBP M2C (Pro), the virus carrying wild-type MLV 4070A env.

elsewhere in the retroviral genome that gives rise to a virus with a “fast” replication phenotype. These results demonstrate that the amino acid residue at position 242 of gp70 has a profound effect on the ability of chimeric RCASBP/MLV env vectors to replicate in avian cells. The data on the replication rates for the mutant viruses are summarized in Table 1.

Infectivities of RCANBP and RCASBP M2C viruses differ depending on the cell type. To determine the relative titers of representatives from each class of Env mutants, we introduced a reporter gene encoding green fluorescent protein (GFP) under the control of an internal CMV promoter into several of the RCANBP M2C viruses. The RCANBP vector differs from RCASBP in that the sequence immediately upstream of the ClaI site, which contains the splice acceptor, has been removed. This means that in the RCANBP M2C (242-mut) CMVgfp vectors, GFP expression is directly under the control of the CMV promoter. There was no difference in replication between the RCASBP M2C (242-mut) and RCANBP M2C (242-mut)CMVgfp viruses in DF-1 cells. Culture supernatants from DF-1 cells infected with RCANBP M2C (242-mut) CMVgfp viruses were applied to 293 cells, and the percentages of fluorescent cells were determined by FACS analysis. These results were normalized to the amount of virus used for each infection, as measured by the level of p27 antigen. Since RCASBP and RCAN vectors do not replicate in mammalian cells, the infection could not spread. Relative to RCANBP M2C (Pro) CMVgfp, which encodes wild-type MLV 4070A Env, RCANBP M2C (4070A) and (797-8) CMVgfp had nearly equivalent titers (39% and 37%, respectively), and RCANBP M2C (Ser)CMVgfp had a titer of 10% (Table 2). As expected, RCASBP(A)gfp was not able to infect 293 cells. Surprisingly, RCANBP M2C (Gln)CMVgfp could not infect 293 cells. In DF-1 cells, RCASBP M2C (Gln) spreads rapidly and replicates as well as RCASBP M2C (4070A) (data not shown). In contrast, RCASBP M2C (Pro) replicates poorly in DF-1 cells (1). However, when the infectivity was corrected for the number of particles, RCANBP M2C (Pro)CMVgfp infected 293 cells more efficiently than either RCANBP M2C (4070A) or (797-8) CMVgfp. Because DF-1 and 293 cells express different versions of the amphotropic receptor, the amino acid at position 242 may affect the efficiency with which amphotropic Env can use the chicken and human forms of the receptor. These results demonstrate that the cell type can profoundly affect the infectivity of the RCANBP and RCASBP M2C viruses.

RCASBP M2C (242-mut) vectors induce different amounts of CPE in DF-1 cells. Infection by the original chimeric vector

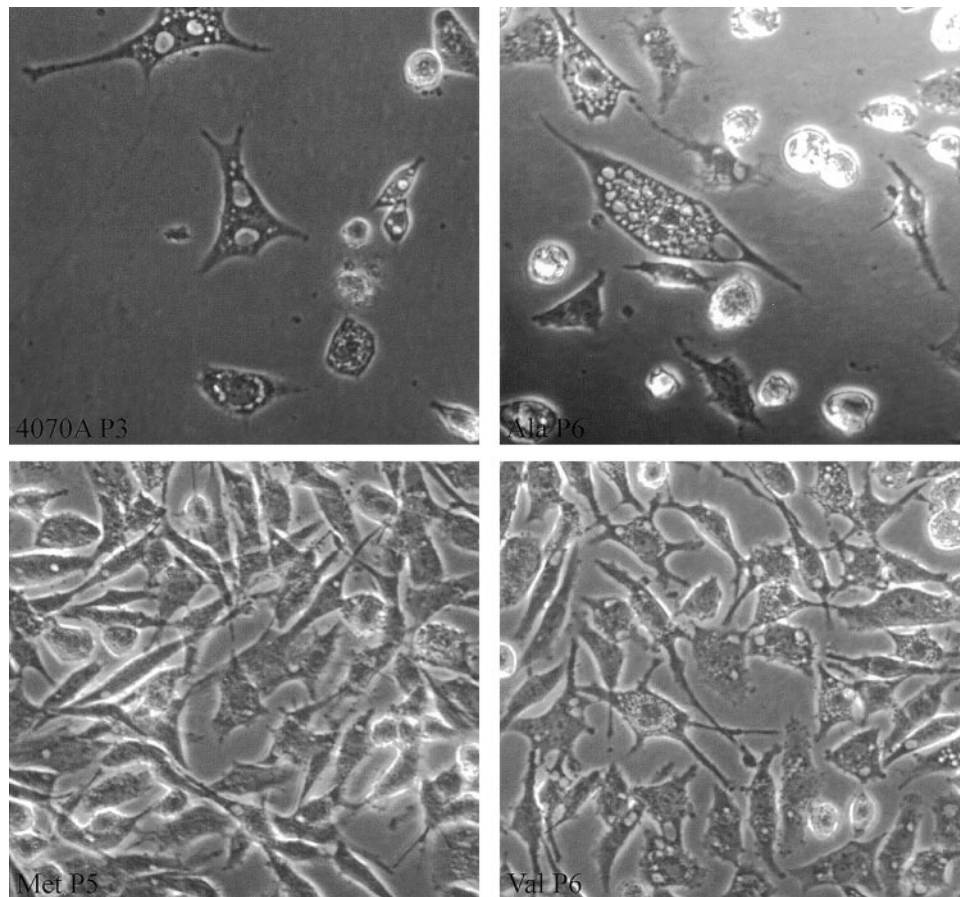


FIG. 3. Representative CPE phenotypes of cells transfected with the RCASBP M2C proviral constructs taken by confocal microscopy. (Top left) High cytotoxicity associated with RCASBP M2C (4070A) at passage 3. (Top right) High cytotoxicity associated with RCASBP M2C (Ala) at passage 6. (Bottom left) Low cytotoxicity associated with RCASBP M2C (Met) at passage 5. (Bottom right) Moderate cytotoxicity associated with RCASBP M2C (Val) at passage 6.

RCASBP M2C (4070A) produced massive CPE in DF-1 cells, causing extensive vacuolization, the formation of syncytia, and cell death. In contrast, the vector RCASBP M2C (797-8), which was obtained by passaging RCASBP M2C (4070A) in chicken embryos, replicated rapidly with minimal CPE. Given the fact that these two viruses differ only in the amino acid residue at position 242, we considered the possibility that both the amount of CPE and the replication rate of the chimeric vectors could be affected by other amino acid substitutions at position 242. The CPE associated with the mutant RCASBP M2C (242-mut) vectors was determined by microscopic observations of infected DF-1 cells. As shown in Fig. 3, the original vector RCASBP M2C (4070A) caused extensive CPE. A similar cytopathology was seen in cells transfected with RCASBP M2C (Ala), (Leu), (Ile), (Glu), (Ser), or (Trp) (Table 1). Some of these viruses had high initial replication rates, i.e., RCASBP M2C (Glu), but other viruses in this group had low initial replication rates. In those cases, it is possible that the high-CPE phenotype may be due to mutations in the codon for amino acid 242 or elsewhere in the *env* gene. In contrast to RCASBP M2C (4070A), mutant viruses such as RCASBP M2C (Thr), RCASBP M2C (His), and RCASBP M2C (Met) induced low cytopathic effects, even in later passages (Fig. 3).

Since each of these viruses exhibited a high initial rate of replication (Table 1), the low CPE could not be attributed to slow replication. A third group of mutants including RCASBP M2C (Arg), RCASBP M2C (Val), and RCASBP M2C (Lys) caused moderate CPE (Fig. 3). A complete summary of these data is found in Table 1.

To quantify the CPE, we measured the total number of cells and the percentage of viable cells during passages of cells infected with viruses that caused high and low CPE based on microscopic observations. There was no difference in the percentage of viable cells or the total number of cells among uninfected, RCASBP M2C (4070A)-infected, and RCASBP M2C (797-8)-infected cells at 2 days postinfection. However, the percentage of dead cells in cultures infected with RCASBP M2C (4070A) was nearly twice as high as that in uninfected or RCASBP M2C (797-8)-infected cells at 4 days (P2) postinfection (Table 3). The total number of cells in RCASBP M2C (4070A)-infected cultures was twofold less than that in (797-8)-infected cultures at P2. Both the number of viable cells and the total number of cells were nearly the same for uninfected DF-1 cultures and (797-8)-infected cultures throughout the time course of infection (Table 2). Overall, the results from the replication rate and CPE measurements indicate that the

TABLE 3. Results of cytotoxicity assay with RCASBP M2C-infected cells^a

Time	Virus	% Dead cells	% Viability	Total cells (cells/ml)
P1	None	5.8 ± 0.35	94.2 ± 0.35	2.6 × 10 ⁶ ± 0.218 × 10 ⁶
	RCASBP M2C (4070A)	7.0 ± 1.47	93.0 ± 1.47	2.4 × 10 ⁶ ± 0.110 × 10 ⁶
	RCASBP M2C (797-8)	6.5 ± 1.07	93.5 ± 1.07	2.3 × 10 ⁶ ± 0.098 × 10 ⁶
P2	None	9.9 ± 0.84	90.1 ± 0.84	1.3 × 10 ⁷ ± 0.190 × 10 ⁷
	RCASBP M2C (4070A)	23.5 ± 0.55	76.5 ± 0.55	5.0 × 10 ⁶ ± 0.250 × 10 ⁶
	RCASBP M2C (797-8)	14.4 ± 3.18	85.6 ± 3.18	1.0 × 10 ⁷ ± 0.332 × 10 ⁷

^a The data are the averages of three independent experiments ± Standard deviations (SD) at P1 (2 days postinfection) and P2 (4 days postinfection).

amino acid residue at position 242 of gp70 strongly affects both parameters but that toxicity does not directly correlate with the replication rate of the virus.

Cells infected with RCASBP M2C (4070A) contain more linear viral DNA than RCASBP M2C (797-1)-infected cells. As previously stated, RCASBP M2C (4070A) causes extensive cell killing in DF-1 cells, whereas RCASBP M2C (797-8) causes low CPE. This difference in CPE led us to address the possible mechanism(s) that could account for the difference. Several reports have noted a correlation, during acute retroviral infection, between the ability to induce CPE and the accumulation of a large amount of unintegrated linear viral DNA (15, 21, 31, 32, 34).

To determine whether the level of virus-induced CPE correlated with the amount of unintegrated linear viral DNA, DF-1 cells were infected with viral stocks generated by transfection. Unintegrated linear viral DNAs were extracted from infected cells by Hirt fractionation and analyzed by Southern blotting. To look specifically for a loss of receptor interference, cells were split 48 h after infection and then plated sparsely. This minimizes opportunities for the viruses produced by infected cells to infect cells that were not previously infected but allows for the reinfection of cells that were already infected if reinfection is not blocked by receptor interference. After two passages, or at 4 days postinfection, a large amount of unintegrated linear viral DNA was present in cells infected with the highly cytopathogenic virus RCASBP M2C (4070A) (Fig. 4A). In comparison, infection with RCASBP M2C (797-8) produced dramatically less unintegrated linear viral DNA. However, infection with RCASBP M2C (797-8) produced more linear viral DNA than was found in RCASBP(A)-infected cells (Fig. 4A). This pattern was consistently seen with these three viruses. The amounts of virus particles produced by RCASBP M2C (4070A)- and RCASBP M2C (797-8)-infected cells were similar at passages 1 and 2 (Table 4), and their relative titers on 293 cells were nearly equivalent (Table 2). Thus, differences in viral titers do not seem to account for the large difference in the amount of unintegrated linear viral DNA seen for cells infected with RCASBP M2C (4070A) and RCASBP M2C (797-8).

Southern blots of extracts of cells infected with RCASBP M2C (Gln), a mutant with moderate to high CPE and a high initial replication rate, showed an intermediate amount of viral linear DNA compared to extracts of cells infected with RCASBP M2C (4070A) and RCASBP M2C (797-8) (Fig. 4B). Unintegrated linear viral DNA was not detectable in cells infected with RCASBP M2C (Ser), a mutant with high CPE but a low initial replication rate, at passage 2 (Fig. 4B). This

result implies that very little infectious virus was present in the RCASBP M2C (Ser) viral stock used to infect the DF-1 cells. Furthermore, it supports the idea that the infectivity of some of the 242 mutants was initially quite low. Additional mutations, either at position 242 or elsewhere within the viral genome, may contribute to the increase in replication rates seen for those mutant viruses with low initial replication rates.

An association between large accumulations of unintegrated retroviral linear DNA and apoptosis has been reported (34). It was suggested that the unintegrated linear viral DNA is perceived as DNA damage by cells and initiates apoptotic signaling. Linear retroviral DNA has been reported to serve as a substrate for the host cell's nonhomologous DNA end-joining pathway that repairs double-strand breaks in cellular DNA (18). However, we were not able to detect an increased number of apoptotic cells in DF-1 cultures infected with RCASBP M2C (4070A) or RCASBP M2C (797-8) within the first three passages, when CPE was obvious (data not shown).

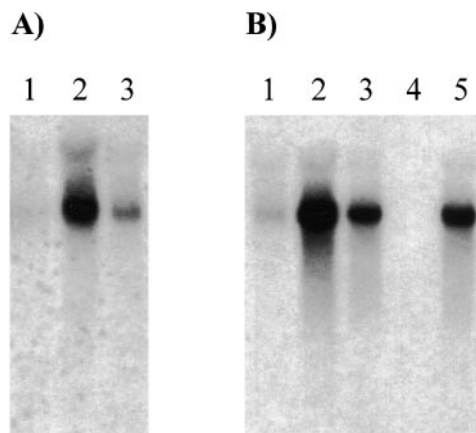


FIG. 4. Southern blots of unintegrated linear viral DNAs from DF-1 cells infected with RCASBP(A) or RCASBP M2C-derived viruses. (A) Relative amounts of unintegrated linear viral DNA isolated by the method of Hirt from RCASBP(A) (lane 1)-, RCASBP M2C (4070A) (lane 2)-, and RCASBP M2C (797-8) (lane 3)-infected cells at passage 2. The blot was probed with ³²P-labeled DNA fragments generated from restriction digests of portions of the RCASBP(A) plasmid, as described in Materials and Methods. (B) Comparison of the relative amounts of linear viral DNA in cells infected with RCASBP(A) and RCASBP M2C-derived viruses with different cytopathic phenotypes. The order of the levels of CPE associated with these viruses, from high to low, are as follows: 4070A (lane 2), Ser (lane 4), Gln (lane 5), 797-8 (lane 3), and RCASBP(A) (lane 1). All of these viruses have high initial replication rates, except for the Ser mutant, which initially replicates slowly (Table 1).

TABLE 4. Levels of p27 antigen in supernatants of infected DF-1 cells

Virus	p27 level ^a	
	Passage 1	Passage 2
None	0.106 ± 0.010	0.100 ± 0.019
RCASBP M2C (797-8)	0.306 ± 0.032	0.434 ± 0.019
RCASBP M2C (4070A)	0.264 ± 0.024	0.441 ± 0.033

^a The data shown are the averages of three independent experiments ± SD. p27 levels were measured by antigen-capture ELISA; the unit of measure is optical density at 450 nm.

Env expression and incorporation in virions. To examine the expression of the RCASBP M2C Env proteins and their incorporation into virions, DF-1 cells were transfected with the representative RCASBP M2C (242-mut) constructs, and the virions produced were pelleted through a 15% sucrose cushion. Western blots showed that the amounts of Env protein in the RCASBP M2C (4070A) and (797-8) virions were similar (Fig. 5A). However, there were modestly reduced amounts of Env incorporated into RCASBP M2C (Gln) virions (Fig. 5A), even though the amounts of Env expressed in the transfected cells for RCASBP M2C (4070A), (797-8), and (Gln) were nearly identical (Fig. 5B). Because the RCASBP M2C (Ser) and RCASBP M2C (Pro) viruses replicated poorly in DF-1 cells, we were not able to detect Env either in the virions (Fig. 5A) or in the transfected cells used to produce them (Fig. 5B). Although p27 was present in the RCASBP M2C (Ser)- and RCASBP M2C (Pro)-transfected cellular lysates (Fig. 5B), the Gag levels were markedly reduced compared to those in (4070A)-, (797-8)-, or (Gln)-transfected cellular lysates.

To determine whether the difference in CPE between RCASBP M2C (4070A) and (797-8) involves disparities in the amounts of Env found on the surfaces of infected cells, the level of Env expression was quantitated by FACS analysis. At

TABLE 5. FACS analysis of cell surface Env expression^a

Virus	Mean fluorescence	p27 antigen level
None	3.56 ± 0.91	0.100 ± 0.019
RCASBP M2C (797-8)	12.00 ± 5.29	0.434 ± 0.019
RCASBP M2C (4070A)	6.99 ± 0.66	0.441 ± 0.033

^a The data shown are the averages of three independent experiments ± SD.

passage 2, cells infected with RCASBP M2C (797-8) had a higher level of Env expression on the cell surface than RCASBP M2C (4070A)-infected cells (Table 5). The increased amount of Env found on the surfaces of RCASBP M2C (797-8)-infected cells was not due to significant differences in the viral titer, since the relative titers, as measured by p27 antigen-capture ELISA, were equivalent (Table 5). Because there was considerable cytotoxicity, the number of RCASBP M2C (4070A)-infected cells at passage 2 was approximately twofold less than the number of RCASBP M2C (797-8)-infected cells (Table 3). Thus, it is possible that the RCASBP M2C (4070A)-infected cells that are still viable at 4 days postinfection are those which have, on average, lower levels of Env expression, while those with higher levels of expression have been eliminated from the culture.

Treatment of RCASBP M2C (4070A)-infected cells with dantrolene reduces the amount of CPE. Several studies have reported changes in the intracellular Ca²⁺ concentration as a trigger for the initiation of cell death (11, 22, 29). The treatment of neuronal cells with dantrolene, a drug that prevents the release of Ca²⁺ from the ER into the cytoplasm by inhibiting ryanodine receptor channels, can protect the cells from death (30). To determine whether the inhibition of Ca²⁺ release from the ER into the cytoplasm could reduce or abrogate the extensive CPE associated with RCASBP M2C (4070A) infection, infected cells were treated with 50 μM dantrolene. In uninfected DF-1 cells, the addition of dantrolene did not produce any observable CPE (Fig. 6A). However, RCASBP M2C (4070A)-infected cells treated with dantrolene had dramatically less vacuolization and were generally more robust than parallel untreated cultures (Fig. 6A). The greatest difference in CPE between untreated and treated RCASBP M2C (4070A)-infected cultures was seen 2 to 3 days after the dantrolene addition. When the drug was removed from these cells, vacuoles began to appear (data not shown). Dantrolene treatment appears to delay the onset of vacuolization in RCASBP M2C (4070A)-infected cells, although syncytia were still observed in infected cells treated with dantrolene. In addition, the amounts of p27 protein found in the supernatants of untreated and treated cells were equivalent when measured by p27 antigen-capture ELISA (Fig. 6B). This result was consistently seen and suggests that dantrolene treatment did not affect virus particle production. We also treated RCASBP(B)-infected DF-1 cells, which show CPE, with dantrolene. The addition of the drug did not cause any observable differences between untreated and treated cells (data not shown). Taken together, our data suggest that the release of calcium from the endoplasmic reticulum plays a role in the CPE seen during RCASBP M2C infection of DF-1 cells.

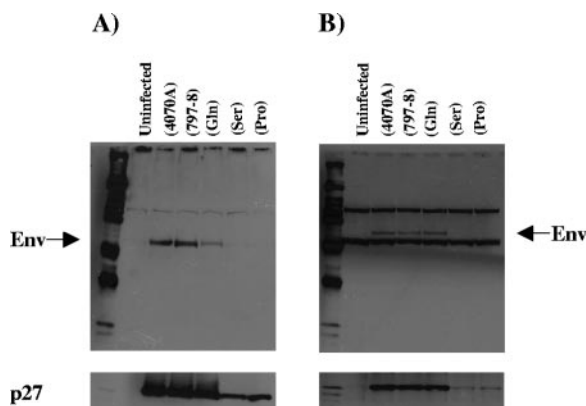


FIG. 5. Env expression and incorporation into RCASBP M2C virions. (A) Western blot of virions pelleted through a 15% sucrose cushion, fractionated in a gel, transferred to a nitrocellulose membrane, and visualized using rabbit anti-gp70 and chemiluminescence. The blots were washed and reprobed with rabbit anti-p27 conjugated to horseradish peroxidase to determine the amount of Gag (bottom panels). The bands shown are the virions released into the supernatants of RCASBP M2C (4070A)-, (797-8)-, (Gln)-, (Ser)-, and (Pro)-transfected DF-1 cell cultures. (B) Western blot of cellular lysates from the transfected cultures used to generate the viruses.

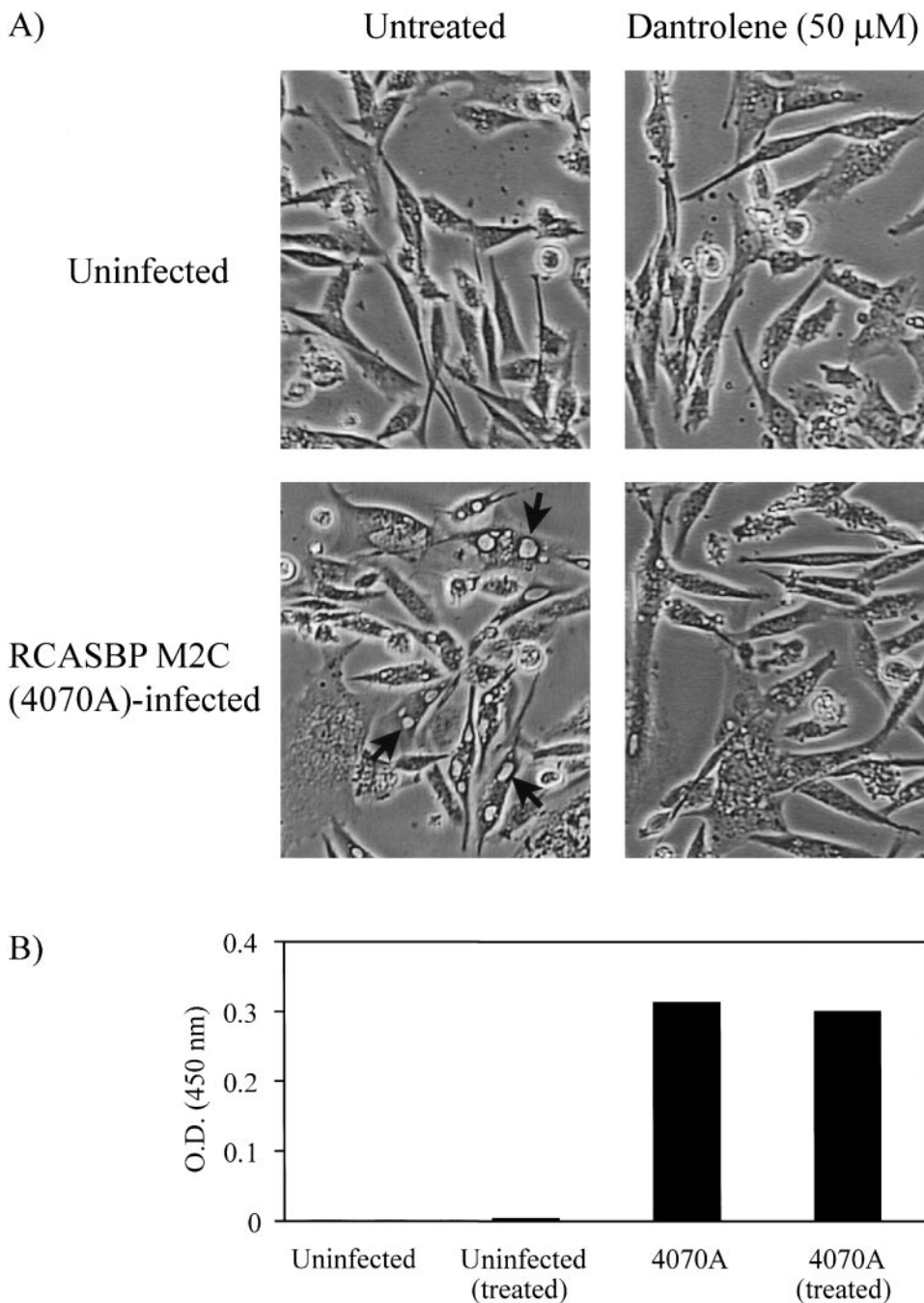


FIG. 6. Effects of dantrolene on uninfected and RCASBP M2C (4070A)-infected cells. (A) Uninfected cells (top panels) and cells infected with RCASBP M2C (4070A) (bottom panels) were either left untreated (left panels) or treated with 50 μ M dantrolene (right panels) for 3 days. The arrows highlight vacuoles seen within cells infected with RCASBP M2C (4070A) that were not treated with dantrolene. (B) Amounts of p27 antigen found in the supernatants of the uninfected or RCASBP M2C (4070A)-infected cells (untreated versus dantrolene-treated) shown in panel A, as measured by p27 antigen-capture ELISA.

DISCUSSION

Previous studies in our laboratory suggested that in RCASBP vectors which replicate using the Env protein of an amphotropic MLV, the amino acid at position 242 of the SU subunit could influence both the replication rate and the amount of CPE (2). For the present study, we introduced various amino acids at position 242 and showed that the nature of the amino acid at this

position profoundly affected the properties of the virus. The dramatic differences in CPE seen with the chimeric mutants led us to investigate the mechanism(s) that could account for the observed differences in the CPE. Since the mutation lies within the PRR of the SU subunit, an obvious explanation would be effects on viral entry due either to differences in the interaction with the receptor and/or membrane fusion.

Several studies have suggested that the PRR has a role in the stability of both the interaction between the SU and TM subunits (10, 16, 33) and the envelope complex (16). Mutations within the PRR increase the shedding of the SU subunit and affect both cell-cell and virus-cell fusion. Lavillette et al. proposed a model in which the PRR stabilizes the SU subunit in the initial (fusion-inactive) state. Upon receptor binding, the stability conferred by the PRR is disrupted, permitting the subsequent events necessary for fusion activation to occur (17). Our data suggest that mutations in the PRR affect the amount of cell-cell fusion in DF-1 cells infected with the chimeric amphotropic viruses. Infection by RCASBP M2C (4070A) and chimeric viruses with moderate or high CPE induced more syncytia than infection by RCASBP M2C (797-8) and the other viruses that caused low CPE (data not shown). Thus, one of the possible mechanisms contributing to the observed differences in cytotoxicity among the chimeric viruses may be a difference in cell-cell fusion and, possibly, virus-cell fusion. The CPE could be a direct result of the interactions between the Env protein and the receptor. However, the most prominent CPE seen in infected cells are vacuolization and cell death. It should be reiterated that the observed CPE caused by some of the chimeric viruses, which had low initial rates of replication, could have resulted from a further mutation of amino acid 242 or secondary mutations elsewhere in the viral genome.

A second explanation for the observed CPE is superinfection of the infected cells, which could be caused by a partial failure of receptor interference. For several retroviruses, including ASLV, superinfection causes CPE during infection (15, 31, 34). This type of effect is usually seen when the target cells are not derived from the natural host of the virus. Presumably, in these cases, the receptor interacts with the envelope protein sufficiently well to permit infection, but the interaction is not sufficient to produce complete receptor interference. In our case, the Env protein is from a murine virus and the receptor is from an avian host. A related RCAS vector system involving the ecotropic MLV envelope protein and modified DF-1 cells that express the murine ecotropic receptor does not cause CPE (2). The original parental virus expressing the wild-type MLV 4070A Env, RCASBP M(4070A), replicated poorly in DF-1 cells and was adapted by serial passages. Because the mutation leading to the adaptation occurred in the SU subunit, we expected to find a change that would affect the interaction with the receptor. Despite the fact that the PRR is not part of the receptor-binding domain of the MLV SU subunit, the PRR has been shown to influence the receptor-binding properties of some MLV subtypes (4, 12), perhaps because the PRR has an effect on the overall structure (33).

The data we obtained comparing the abilities of the mutant viruses to spread in DF-1 cells and their relative titers (corrected for the amount of p27) on 293 cells also suggest that the mutations at position 242 differentially affect the specificity of the interactions of the SU subunit with the avian receptor in DF-1 cells and the human receptor in 293 cells. Some of the viruses that spread rapidly and efficiently in DF-1 cells were poorly infectious on 293 cells. Conversely, some of the viruses that spread slowly in DF-1 cells infected 293 cells efficiently. The idea that the mutations at position 242 directly affect the specificity of the interaction with SU is supported by the ob-

ervation that the various mutants differed in the ability to cause receptor interference. However, the ability of the mutant viruses to replicate on DF-1 cells does not correlate with their ability to cause receptor interference. This suggests that a less stringent interaction between SU and the receptor is needed for efficient viral replication than is needed for a high level of receptor interference, at least in cell culture. If this is also true *in vivo*, it would suggest that one of the critical forces selecting for the very tight binding between SU and its cognate receptor, which is found in naturally occurring viruses, is the need for effective receptor interference.

The lack of effective receptor interference allows for superinfection, and one of the hallmarks of superinfection is the accumulation of large amounts of unintegrated linear retroviral DNA. Early studies with spleen necrosis virus and ASLV suggested that there is a correlation between CPE and an accumulation of linear retroviral DNA during acute infection (15, 31). We also saw a correlation between the amount of CPE and the accumulation of unintegrated linear retroviral DNA. DF-1 cells infected with the highly cytotoxic virus, RCASBP M2C (4070A), accumulated large amounts of linear viral DNA. There was an intermediate accumulation of viral DNA following infection with a virus that causes moderate to high CPE [RCASBP M2C(Gln)]. The amount of linear viral DNA produced during infection by the low-CPE virus, RCASBP M2C (797-8), was lower still (Fig. 4A). These results suggest that receptor interference is incomplete for RCASBP M2C (4070A) and for the other amphotropic chimeric viruses which cause moderate to high CPE. The amount of linear retroviral DNA was lower in RCASBP(A)-infected cells than in RCASBP M2C (797-8)-infected cells, suggesting that receptor interference was still not complete even in cells infected with the low-CPE chimeric viruses.

Yoshimura et al. proposed a model whereby the accumulated unintegrated linear retroviral DNA is perceived as DNA damage by the infected cells and induces apoptosis (34). Extensive cell death is observed during RCASBP M2C (4070A) infection. However, we did not detect an induction of apoptosis during RCASBP M2C (4070A) infection (data not shown). Another possibility is that the cell death associated with RCASBP M2C (4070A) infection occurs through necrosis. One phenotype of necrotic cells is extensive vacuolization of the cytoplasm (29).

Necrosis can be initiated by several cellular stresses, including the perturbation of ion homeostasis, *i.e.*, changes in the intracellular Ca^{2+} concentration (29). The endoplasmic reticulum has the largest store of Ca^{2+} in the cell, and disturbances of the calcium homeostasis in this organelle can affect intracellular calcium concentrations and initiate cell death through the necrotic and/or apoptotic pathway (22, 29). Calcium influx into the ER occurs via sarco(endo)plasmic reticulum Ca^{2+} -ATPase pumps, and calcium efflux from the ER into the cytoplasm occurs through inositol-1,4,5-triphosphate [$\text{Ins}(1,4,5)\text{P}_3$] and ryanodine receptors (22). The release of calcium from the ER into the cytoplasm activates several calcium-dependent proteases involved in both the necrotic and apoptotic pathways (22, 29). The drug dantrolene can prevent the release of calcium from the ER by inhibiting ryanodine receptors. Dantrolene treatment of neuronal cells can protect against chemically induced cell death (30). When RCASBP M2C (4070A)-

infected cells were treated with 50 μ M dantrolene for 3 days, dramatically less vacuolization was seen than that in untreated control cells. The treated cells also appeared to be more robust (Fig. 6A). However, upon removal of the drug, the infected cells began to show increased vacuolization, suggesting that the effect of the drug on the onset of CPE was reversible and that removing the drug allowed the release of calcium and the development of CPE. We cannot rule out the possibility that dantrolene treatment indirectly affects other cellular or viral processes, since calcium plays a part in several important pathways. However, uninfected DF-1 cells treated with dantrolene did not appear to be different from the untreated control cells, indicating that the concentration of the drug used in these experiments did not adversely affect DF-1 cells (Fig. 6A). Furthermore, the amount of p27 protein found in the supernatant of dantrolene-treated, RCASBP M2C (4070A)-infected cells was equivalent to that in the supernatant of untreated controls (Fig. 6B), suggesting that virus production was not affected by dantrolene treatment. Taken together, these results indicate that the release of calcium from the endoplasmic reticulum plays a role in the CPE seen during infection.

We propose the following model to explain how CPE arise during infections of DF-1 cells by our chimeric RCASBP M2C vectors. Initially, interactions of a partially mismatched Env and receptor cause incomplete or attenuated receptor interference. This allows for repeated reinfections of previously infected cells. The cellular stresses that result from superinfection, which could involve interactions between Env and the receptor as well as the accumulation of unintegrated linear viral DNA, lead to cell death. The induced cell death potentially occurs through the necrotic pathway. Necrosis is triggered, at least in part, by the release of calcium from the ER stores and is characterized by extensive vacuolization.

ACKNOWLEDGMENTS

We thank Leonard Evans for kindly providing the 83A25 monoclonal antibody and Monica Roth for technical help with the preparation of 83A25 for FACS analysis. We also thank Louise Finch for FACS analysis and Hilda Marusiodis for help with preparing the manuscript.

Research in the laboratory of S.H.H. was supported by the National Cancer Institute and by the National Institute for General Medical Sciences.

REFERENCES

- Barsov, E. V., and S. H. Hughes. 1996. Gene transfer into mammalian cells by a Rous sarcoma virus-based retroviral vector with the host range of the amphotropic murine leukemia virus. *J. Virol.* **70**:3922–3929.
- Barsov, E. V., W. S. Payne, and S. H. Hughes. 2001. Adaptation of chimeric retroviruses in vitro and in vivo: isolation of avian retroviral vectors with extended host range. *J. Virol.* **75**:4973–4983.
- Bates, P., J. A. T. Young, and H. E. Varmus. 1993. A receptor for subgroup A Rous sarcoma virus is related to the low density lipoprotein receptor. *Cell* **74**:1043–1051.
- Battini, J. L., J. M. Heard, and O. Danos. 1992. Receptor choice determinants in the envelope proteins of amphotropic, xenotropic, and polytropic murine leukemia viruses. *J. Virol.* **66**:1468–1475.
- Brojatsch, J., J. Naughton, M. M. Rolls, K. Zingler, and J. A. T. Young. 1996. CAR1, a TNFR-related protein, is a cellular receptor for cytopathic avian leukemia-sarcoma viruses and mediates apoptosis. *Cell* **87**:845–855.
- Diaz-Griffero, F., S. A. Hoschander, and J. Brojatsch. 2003. Bystander killing during avian leukemia virus subgroup B infection requires TVB^{S3} signaling. *J. Virol.* **77**:12552–12561.
- Evans, L. H., R. P. Morrison, F. G. Malik, J. Portis, and W. Britt. 1990. A neutralizable epitope common to the envelope glycoprotein of ecotropic, polytropic, xenotropic, and amphotropic murine leukemia viruses. *J. Virol.* **64**:6176–6183.
- Federspiel, M. J., and S. H. Hughes. 1997. Retroviral gene delivery. *Methods Cell Biol.* **52**:179–214.
- Graham, F. L., and A. J. van der Eb. 1973. A new technique for the assay of infectivity of human adenovirus 5 DNA. *Virology* **52**:456–467.
- Gray, K. D., and M. J. Roth. 1993. Mutational analysis of the envelope gene of Moloney murine leukemia virus. *J. Virol.* **67**:3489–3496.
- Hajnóczky, G., E. Davies, and M. Madesh. 2003. Calcium signaling and apoptosis. *Biochem. Biophys. Res. Commun.* **304**:445–454.
- Han, J.-Y., P. M. Cannon, K.-M. Lai, Y. Zhao, M. V. Eiden, and W. F. Anderson. 1997. Identification of envelope protein residues required for the expanded host range of 10A1 murine leukemia virus. *J. Virol.* **71**:8103–8108.
- Himly, M., D. N. Foster, I. Bottoli, J. S. Iacovoni, and P. K. Vogt. 1998. The DF-1 chicken fibroblast cell line: transformation induced by diverse oncogenes and cell death resulting from infection by avian leukosis viruses. *Virology* **248**:295–304.
- Hirt, B. 1967. Selective extraction of polyoma DNA from infected mouse cell cultures. *J. Mol. Biol.* **26**:365–369.
- Keshet, E., and H. M. Temin. 1979. Cell killing by spleen necrosis virus is correlated with a transient accumulation of spleen necrosis virus DNA. *J. Virol.* **31**:376–388.
- Lavillette, D., M. Maurice, C. Roche, S. J. Russell, M. Sitbon, and F.-L. Cosset. 1998. A proline-rich motif downstream of the receptor binding domain modulates conformation and fusogenicity of murine retroviral envelopes. *J. Virol.* **72**:9955–9965.
- Lavillette, D., A. Ruggieri, B. Boson, M. Maurice, and F.-L. Cosset. 2002. Relationship between SU subdomains that regulate the receptor-mediated transition from the native (fusion-inhibited) to the fusion-active conformation of the murine leukemia virus glycoprotein. *J. Virol.* **76**:9673–9695.
- Li, L., J. M. Olvera, K. E. Yoder, R. S. Mitchell, S. L. Butler, M. Lieber, S. L. Martin, and F. D. Bushman. 2001. Role of the non-homologous DNA end joining pathway in the early steps of retroviral infection. *EMBO J.* **20**:3272–3281.
- Lu, C.-W., and M. J. Roth. 2001. Functional characterization of the N termini of murine leukemia virus envelope proteins. *J. Virol.* **75**:4357–4366.
- Lu, C.-W., and M. J. Roth. 2003. Role of the mutation Q252R in activating membrane fusion in the murine leukemia virus surface envelope protein. *J. Virol.* **77**:10841–10849.
- Mullins, J. L., C. S. Chen, and E. A. Hoover. 1986. Disease-specific and tissue-specific production of unintegrated feline leukemia virus variant DNA in feline AIDS. *Nature* **319**:333–336.
- Orrenius, S., B. Zhivotovsky, and P. Nicotera. 2003. Regulation of cell death: the calcium-apoptosis link. *Nat. Rev. Mol. Biol.* **4**:552–565.
- Orsulic, S. 2002. An RCAS-TVA-based approach to designer mouse models. *Mamm. Genome* **13**:543–547.
- Pao, W., D. S. Klimstra, G. H. Fisher, and H. E. Varmus. 2003. Use of avian retroviral vectors to introduce transcriptional regulators into mammalian cells for analyses of tumor maintenance. *Proc. Natl. Acad. Sci. USA* **100**:8764–8769.
- Pauza, C. D., J. E. Galindo, and D. D. Richman. 1990. Reinfection results in accumulation of unintegrated viral DNA in cytopathic and persistent human immunodeficiency virus type 1 infection of CEM cells. *J. Exp. Med.* **172**:1035–1042.
- Pinter, A., W. J. Honnen, J.-S. Tung, P. V. O'Donnell, and U. Hammerling. 1982. Structural domains of endogenous murine leukemia virus gp70s containing specific antigenic determinants defined by monoclonal antibodies. *Virology* **116**:499–516.
- Robinson, H. L., and D. M. Zinkus. 1990. Accumulation of human immunodeficiency virus type 1 DNA in T cells: result of multiple infection events. *J. Virol.* **64**:4836–4851.
- Schaefer-Klein, J., I. Givol, E. V. Barsov, J. M. Whitcomb, M. VanBroeklin, D. N. Foster, M. J. Federspiel, and S. H. Hughes. 1998. The EV-O-derived cell line DF-1 supports the efficient replication of avian leukosis-sarcoma viruses and vectors. *Virology* **248**:305–311.
- Syntichaki, P., and N. Tavernarakis. 2003. The biochemistry of neuronal necrosis: rogue biology? *Nat. Rev. Neurobiol.* **4**:672–684.
- Wei, H., P. Leeds, R.-W. Chen, W. Wei, Y. Leng, D. E. Bredesen, and D.-M. Chuang. 2000. Neuronal apoptosis induced by pharmacological concentrations of 3-hydroxykynurenine: characterization and protection by dantrolene and Bcl-2 overexpression. *J. Neurochem.* **75**:81–90.
- Weller, S. K., A. E. Joy, and H. M. Temin. 1980. Correlation between cell killing and massive second-round superinfection by members of some subgroups of avian leukosis virus. *J. Virol.* **33**:494–506.
- Weller, S. K., and H. M. Temin. 1981. Cell killing by avian leukosis viruses. *J. Virol.* **39**:713–721.
- Wu, B. W., P. M. Cannon, E. M. Gordon, F. L. Hall, and W. F. Anderson. 1998. Characterization of the proline-rich region of murine leukemia virus envelope protein. *J. Virol.* **72**:5383–5391.
- Yoshimura, F. K., T. Wang, and S. Nanua. 2001. Mink cell focus-forming murine leukemia virus killing of mink cells involves apoptosis and superinfection. *J. Virol.* **75**:6007–6015.